Spreading Properties of a Lorentz-Gauss Vortex Beam Propagating in Biological Tissues

Dajun Liu*, Hongming Yin, Guiqiu Wang, Aiyi Dong, and Yaochuan Wang

Abstract—The propagation equation of a Lorentz-Gauss (LG) vortex beam in biological tissues is derived. The influences of the beam parameters and the biological tissues on the spreading properties of a LG vortex beam are investigated. The obtained results are interpreted numerically and shown that the LG vortex beam propagating through biological tissues with the stronger turbulence strength will lose the dark hollow center and evolve into the Gaussian-like beam more rapidly.

1. INTRODUCTION

Today, the properties of electromagnetic beams have been investigated, which are used in different contexts, such as twisted electromagnetic waves in plasma [1, 2]. On the other hand, optical waves are also electromagnetic waves. The properties of laser beams have been given in the past years. In the description of the output of lasers, the output of laser diode has been described by using Lorentz beams [3]. Since then, Zhao and Cai have studied the propagation properties of Lorentz and Lorentz-Gauss beams in uniaxial crystals [4]. Liu et al. have investigated the properties of Lorentz beam propagating in oceanic turbulence [5]. Yu et al. have investigated the nonparaxial propagation of Lorentz and Lorentz-Gauss beams in free space [6]. Zhou and Chu have studied the spreading of a Lorentz-Gauss beam in turbulent atmosphere [7]. Du et al. have studied the properties of Lorentz and Lorentz-Gauss beams through a fractional Fourier transform optical system [8]. Zhou and Chen have obtained the Wigner distribution function of Lorentz and Lorentz-Gauss beams propagating through a paraxial ABCD optical system [9]. Liu et al. have studied the nonparaxial propagation of a partially coherent Lorentz-Gauss beam in free space [10]. Liu et al. have investigated the propagation properties of partially coherent Lorentz-Gauss beam propagating through oceanic turbulence [11]. Ni and Zhou have studied the nonparaxial propagation properties of a Lorentz-Gauss vortex beam through uniaxial crystals [12]. Zhou et al. have investigated orbital angular of a linearly polarized Lorentz-Gauss vortex beam [13]. Zhou and Ru have also investigated the propagation properties of a Lorentz-Gauss vortex beam in strongly nonlocal nonlinear media [14]. The orbital angular density of a general Lorentz-Gauss vortex beam has also been obtained [15]. The properties of partially coherent Lorentz-Gauss vortex beams propagating through oceanic turbulence and uniaxial crystal have also been studied by Liu et al. [16, 17]. With the development of biomedical optics, the propagation properties of laser beam in biological tissues have also been studied. Liu and Zhao have studied the properties of anisotropic electromagnetic beams passing through biological tissues [18]. Luo et al. have studied the propagating properties of stochastic electromagnetic vortex beams through turbulent biological tissues [19]. Lu et al. have investigated the propagation properties of anomalous hollow beams in biological tissues [20]. Liu et al. have investigated the propagation properties of anomalous hollow vortex beams in biological tissues [21]. However, to our knowledge, the influences of biological tissues on Lorentz-Gauss (LG) vortex beam have not been reported. In this paper, we investigate the propagation properties of an LG vortex beam in biological tissues.

2. PROPAGATION ANALYSIS OF LG VORTEX BEAM IN BIOLOGICAL TISSUE

In a Cartesian coordinate system, the z-axis is set as the propagation axis, based on the extended Huygens-Fresnel diffraction integral, and the average intensity of laser beams propagating in biological tissues at the receiver plane z can be written as [18–21]:

$$\langle I(\mathbf{r}, z)\rangle = \frac{k^2}{4\pi^2 z^2} \iiint \int\limits_{-\infty}^{+\infty} d\mathbf{r}_{10} d\mathbf{r}_{20} E(\mathbf{r}_{10}, 0) E^*(\mathbf{r}_{20}, 0)$$

$$\times \exp\left[-\frac{ik}{2z}(\mathbf{r} - \mathbf{r}_{10})^2 + \frac{ik}{2z}(\mathbf{r} - \mathbf{r}_{20})^2\right] \langle \exp[\psi(\mathbf{r}_{10}, \mathbf{r}) + \psi^*(\mathbf{r}_{20}, \mathbf{r})]\rangle. \tag{1}$$

where $\langle I(\mathbf{r}, z)\rangle$ is the average intensity of laser beam at the receiver plane z; $k = 2\pi/\lambda$ denotes the wave number; λ denotes the wavelength; asterisk denotes the complex conjugation; $\psi(\mathbf{r}_0, \mathbf{r}, z)$ is the random part of complex phase of a spherical wave propagating in biological tissues. The last term at Equation (1) can be expressed as:

$$\langle \exp[\psi(\mathbf{r}_{10}, \mathbf{r}) + \psi^*(\mathbf{r}_{20}, \mathbf{r})]\rangle = \exp\left[-\frac{(x_{10} - x_{20})^2 + (y_{10} - y_{20})^2}{\rho_0^2}\right], \tag{2}$$

where $\rho_0 = 0.22 \times \left(C_n^2 k^2 z\right)^{-1/2}$ is the coherence length of a spherical wave propagating in biological tissues and C_n^2 the constant of refractive index structure of biological tissues.

LG beam has been introduced to describe the output of laser diode [3], and LG vortex beam has been given to describe the LG beam with angular momentum in previous reports [12, 14, 15]. The optical field of an LG vortex beam at the source plane $z = 0$ can be written as:

$$E(\mathbf{r}_0, 0) = \frac{w_{0x} w_{0y}}{\left(w_{0x}^2 + x_0^2\right)\left(w_{0y}^2 + y_0^2\right)} \exp\left(-\frac{x_0^2 + y_0^2}{w_0^2}\right)(x_0 + iy_0)^M, \tag{3}$$

where $\mathbf{r}_0 = (x_0, y_0)$ is the position vector at the source plane $z = 0$; w_{0x} and w_{0y} are the parameters related to the beam widths of the Lorentz part of the LG vortex beam in the x and y directions, respectively; w_0 is the waist width of the Gaussian part of the LG vortex beam; M is the topological charge of LG vortex beam. The topological term in Equation (3) can be expressed as [22]:

$$(x + iy)^M = \sum_{l=0}^{M} \frac{M! i^l}{l!(M - l)!} x^{M-l} y^l. \tag{4}$$

By substituting Equation (5) into Equation (1) and recalling the following integral equations [22, 23]:

$$\int_{-\infty}^{+\infty} x^n \exp\left(-px^2 + 2qx\right) dx = n! \exp\left(\frac{q^2}{p}\right)\left(\frac{q}{p}\right)^n \sqrt{\frac{\pi}{p}} \sum_{k=0}^{[n/2]} \frac{1}{k!(n - 2k)!}\left(\frac{p}{4q^2}\right)^k, \tag{5}$$

$$\frac{1}{\left(x^2 + w_{0x}^2\right)\left(y^2 + w_{0y}^2\right)} = \frac{\pi}{2w_{0x}^2 w_{0y}^2} \sum_{m=0}^{N} \sum_{n=0}^{N} \sigma_{2m} \sigma_{2n} H_{2m}\left(\frac{x}{w_{0x}}\right) H_{2n}\left(\frac{y}{w_{0y}}\right) \times \exp\left(-\frac{x^2}{2w_{0x}^2} - \frac{y^2}{2w_{0y}^2}\right), \tag{6}$$

$$H_{2m}(x) = \sum_{l=0}^{m} \frac{(-1)^l (2m)!}{l!(2m - 2l)!}(2x)^{2m-2l}. \tag{7}$$

In Equation (6), N is the number of the expansions; σ_{2m} and σ_{2n} are the expanded coefficients which can be found in [23].

After some tedious calculation, the following equations can be derived

$$I(\mathbf{r}, z) = \frac{k^2}{16 w_{0x}^2 w_{0y}^2 z^2} \sum_{m1=0}^{N} \sum_{n1=0}^{N} \sum_{m2=0}^{N} \sum_{n2=0}^{N} \sigma_{2m1} \sigma_{2n1} \sigma_{2m2} \sigma_{2n2} \sum_{l1=0}^{M} \frac{M! i^{l1}}{l1!(M - l1)!} \sum_{l2=0}^{M} \frac{M!(-i)^{l2}}{l2!(M - l2)!} \times I_x I_y. \tag{8}$$

where

$$
\begin{aligned}
I_x = \ & \exp\left(-\frac{k^2}{4a_x z^2}x^2\right) \sum_{t=0}^{m1} \frac{(-1)^t (2m1)!}{t!(2m1-2t)!} \left(\frac{2}{w_{0x}}\right)^{2m1-2l} \sqrt{\frac{\pi}{a_{x1}}}\,(M-l1+2m1-2t)! \\
& \times \left(\frac{1}{a_x}\right)^{(M-l1+2m1-2t)} \sum_{s=0}^{\left[\frac{M-l1+2m1-2t}{2}\right]} \frac{1}{s!(M-l1+2m1-2t-2s)!} \left(\frac{a_x}{4}\right)^s \\
& \times \sum_{e=0}^{M-l1+2m1-2t-2s} \frac{(M-l1+2m1-2t-2s)!}{e!(M-l1+2m1-2t-2s-e)!} \left(\frac{ik}{2z}x\right)^{M-l1+2m1-2t-2s-e} \left(\frac{1}{\rho_0^2}\right)^e \\
& \times \sum_{h=0}^{m2} \frac{(-1)^h (2m2)!}{h!(2m2-2h)!} \left(\frac{2}{w_{0x}}\right)^{2m2-2h} \sqrt{\frac{\pi}{b_x}} 2^{-(M-l2+e+2m2-2h)} i^{M-l2+e+2m2-2h} \\
& \times \left(\frac{1}{b_x}\right)^{0.5(M-l2+e+2m2-2h)} \exp\left(\frac{c_x^2}{b_x}x^2\right) H_{M-l2+e+2m2-2h}\left(-\frac{ic_x}{\sqrt{b_x}}x\right)
\end{aligned} \tag{9}
$$

$$
\begin{aligned}
I_y = \ & \exp\left(-\frac{k^2}{4a_y z^2}y^2\right) \sum_{t=0}^{n1} \frac{(-1)^t (2n1)!}{t!(2n1-2t)!} \left(\frac{2}{w_{0y}}\right)^{2n1-2l} \sqrt{\frac{\pi}{a_y}}\,(l1+2n1-2t)! \\
& \times \left(\frac{1}{a_y}\right)^{(l1+2n1-2t)} \sum_{s=0}^{\left[\frac{l1+2n1-2t}{2}\right]} \frac{1}{s!(l1+2n1-2t-2s)!} \left(\frac{a_y}{4}\right)^s \\
& \times \sum_{e=0}^{l1+2n1-2t-2s} \frac{(l1+2n1-2t-2s)!}{e!(l1+2n1-2t-2s-e)!} \left(\frac{ik}{2z}y\right)^{l1+2n1-2t-2s-e} \left(\frac{1}{\rho_0^2}\right)^e \\
& \times \sum_{h=0}^{n2} \frac{(-1)^h (2n2)!}{h!(2n2-2h)!} \left(\frac{2}{w_{0y}}\right)^{2n2-2h} \sqrt{\frac{\pi}{b_y}} 2^{-(l2+e+2n2-2h)} i^{l2+e+2n2-2h} \\
& \times \left(\frac{1}{b_y}\right)^{0.5(l2+e+2n2-2h)} \exp\left(\frac{c_y^2}{b_y}y^2\right) H_{l2+e+2n2-2h}\left(-\frac{ic_y}{\sqrt{b_y}}y\right)
\end{aligned} \tag{10}
$$

where

$$
a_\alpha = \frac{1}{2w_{0\alpha}^2} + \frac{1}{w_0^2} + \frac{1}{\rho_0^2} + \frac{ik}{2z} \ (\alpha = x, y), \tag{11}
$$

$$
b_\alpha = \frac{1}{2w_{0\alpha}^2} + \frac{1}{w_0^2} + \frac{1}{\rho_0^2} - \frac{ik}{2z} - \frac{1}{a_\alpha}\left(\frac{1}{\rho_0^2}\right)^2, \tag{12}
$$

$$
c_\alpha = \left(\frac{1}{a_\alpha \rho_0^2} - 1\right)\frac{ik}{2z}. \tag{13}
$$

3. NUMERICAL RESULTS AND DISCUSSION

In this section, the spreading properties of an LG vortex beam propagating through biological tissues at the receiver plane z are investigated by using numerical examples. In numerical calculations, the parameters of source beam are set as $\lambda = 0.8\,\mu m$, $w_0 = 40\,\mu m$, $M = 1$, and $N = 5$ (the expanded coefficients σ_{2m} and σ_{2n} decrease faster, so N will not be large in numerical calculations) without other explanation.

In the following analyses, the samples of biological tissues are chosen as upper dermis of human ($C_n^2 = 0.44 \times 10^{-3}\,\mu m^{-1}$), deep dermis of mouse ($C_n^2 = 0.22 \times 10^{-3}\,\mu m^{-1}$), and the intestinal epithelium of mouse ($C_n^2 = 0.6 \times 10^{-4}\,\mu m^{-1}$) [18, 24].
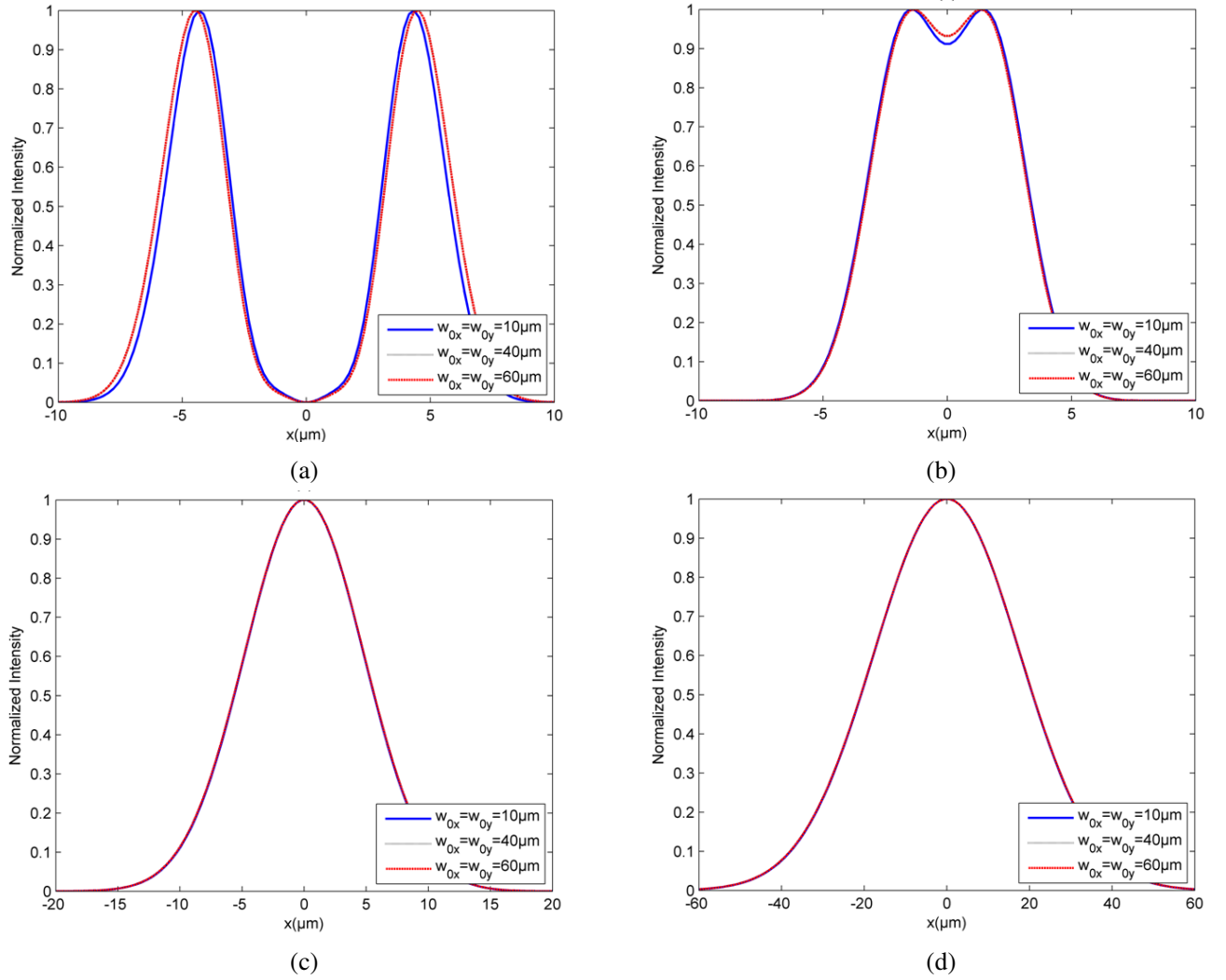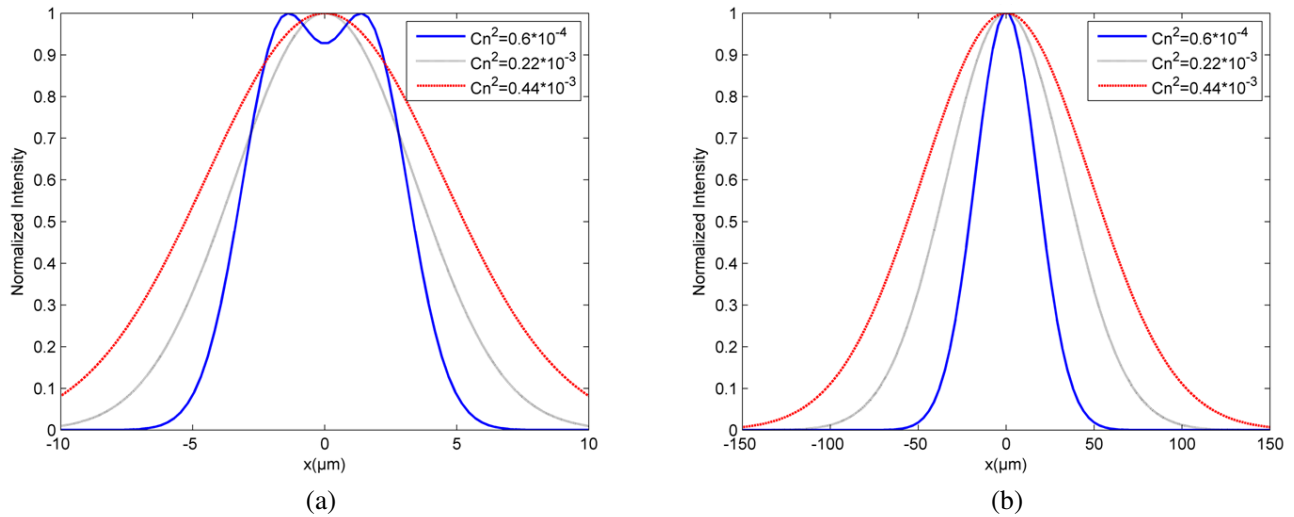
Figure 1. Cross sections of normalized average intensity of a LG vortex beam with M=1 propagating in biological tissues with $C_n^2 = 0.6 \times 10^{-4} \mu\text{m}^{-2/3}$ for the different $w_{0x} = w_{0y}$. (a) $z = 0.5 \, \mu\text{m}$, (b) $z = 10 \, \mu\text{m}$, (c) $z = 20 \, \mu\text{m}$, (d) $z = 50 \, \mu\text{m}$.

The cross sections of normalized average intensity for an LG vortex beam with $M = 1$ propagating in the biological tissues with $C_n^2 = 0.6 \times 10^{-4} \, \mu\text{m}^{-1}$ (intestinal epithelium of mouse) for different $w_{0x} = w_{0y}$ are shown in Figure 1. From Figure 1(a), it is found that an LG vortex beam with smaller $w_{0x} = w_{0y}$ will have a smaller beam spot at short propagation distance (blue line). As the propagation distance increases, the LG vortex beam will lose the dark hollow center introduced by M, and the LG vortex beam with larger $w_{0x} = w_{0y}$ will lose the dark hollow center faster (red line). As the propagation distance increases, the LG vortex beam with different $w_{0x} = w_{0y}$ will all evolve from dark hollow center beam into the Gaussian-like beam affected by the biological tissues, while the influences of different $w_{0x} = w_{0y}$ on the beam spot are not so evident at a sufficiently long propagation distance (Figure 1(d)). The reason is that the LG vortex beam with smaller $w_{0x} = w_{0y}$ will spread faster as the propagation distance increases, thus the LG vortex beam with smaller $w_{0x} = w_{0y}$ can have the same beam pot as the LG vortex beam with larger $w_{0x} = w_{0y}$ with the increase of propagation distance z.

Figure 2 illustrates the cross sections of normalized average intensity for an LG vortex beam with $w_{0x} = w_{0y} = 10 \, \mu\text{m}$ propagating through the biological tissues with $C_n^2 = 0.6 \times 10^{-4} \, \mu\text{m}^{-1}$ for different M. From Figure 2, one finds that the LG vortex beam with larger M will have a larger dark hollow center at the short propagation distance, and the LG vortex beam with different M propagating in

(a)

(b)
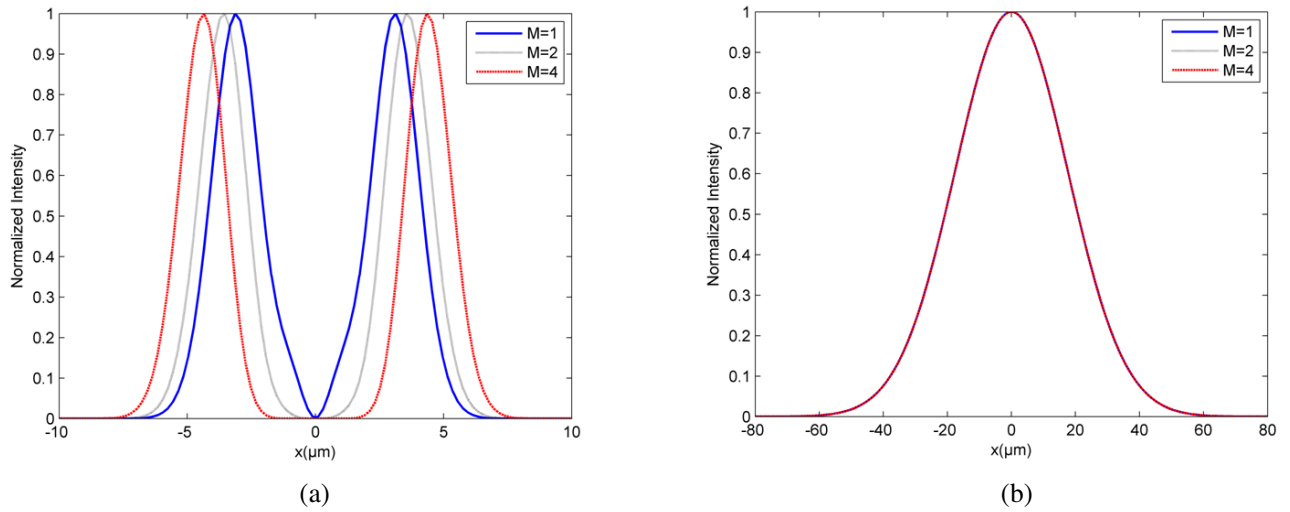
Figure 2. Cross sections of normalized average intensity of a LG vortex beam with $w_{0x} = w_{0y} = 10\,\mu m$ propagating in biological tissueswith $C_n^2 = 0.6 \times 10^{-4}\,\mu m^{-2/3}$ for the different M. (a) $z = 1\,\mu m$, (b) $z = 50\,\mu m$.
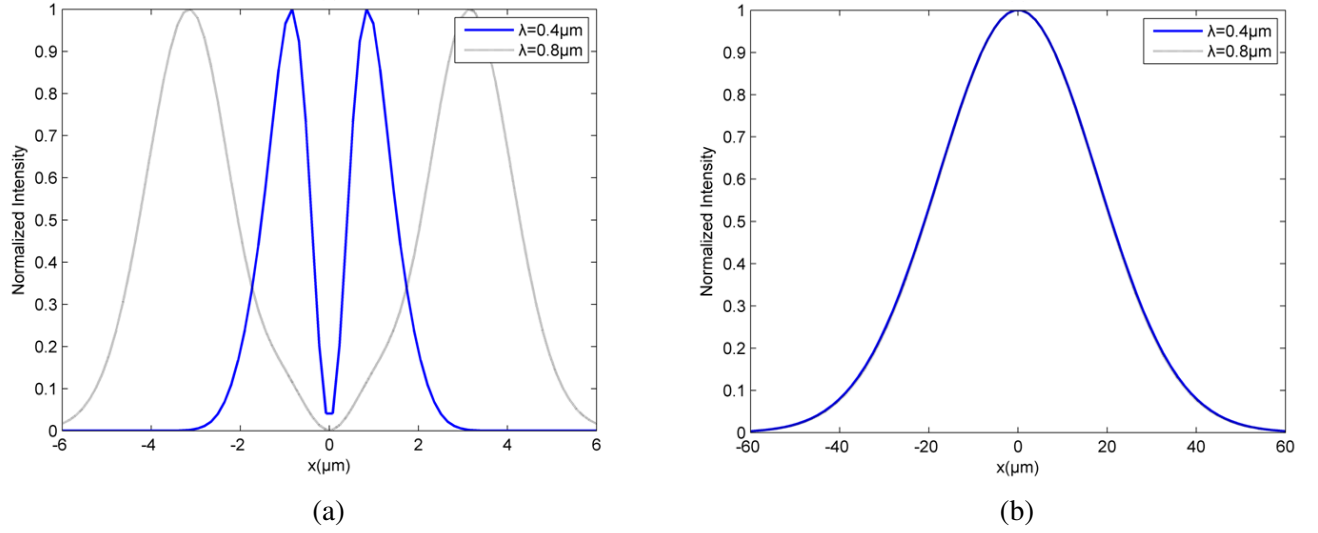

(a)

(b)

Figure 3. Cross sections of normalized average intensity of a LG vortex beam with $M = 1$ propagating in biological tissuesfor the different C_n^2. (a) $z = 10\,\mu m$, (b) $z = 50\,\mu m$.

biological tissues will evolve into a Gaussian-like beam with a similar beam spot (Figure 2(b)).

The cross sections of normalized average intensity for an LG vortex beam with $w_{0x} = w_{0y} = 20\,\mu m$ and $M = 1$ propagating in the biological tissues for the different C_n^2 are given in Figure 3. It is found that the LG vortex beam propagating in biological tissues with larger C_n^2 will lose the dark hollow center and evolve into a Gaussian-like beam at the short propagation distance (Figure 3(a)). As the propagation distance increases, the LG vortex beam propagating in biological tissues with smaller C_n^2 will also evolve into a Gaussian-like beam. This can be explained as that the turbulence strength of the biological tissues will become stronger with increasing C_n^2.

Figure 4 shows the cross sections of normalized average intensity for a LG vortex beam with $w_{0x} = w_{0y} = 20\,\mu m$ and $M = 1$ propagating in the biological tissues with $C_n^2 = 0.6 \times 10^{-4}\,\mu m^{-1}$ for different λ. One can see that the Lorentz-Gauss vortex beam with smaller λ will have a smaller beam spot at the short distance. On the other hand, the influence of different wavelengths λ on spreading

Figure 4. Cross sections of normalized average intensity of a LG vortex beam with $M = 1$ propagating in biological tissues for the different λ. (a) $z = 1\,\mu\text{m}$, (b) $z = 50\,\mu\text{m}$.

of the beam propagating through biological tissues will disappear at a longer propagation distance (Figure 4(b)).

4. CONCLUSIONS

Based on the Huygens-Fresnel integral, the model of an LG vortex beam applied in biological tissues has been described; the analytical equation of an LG vortex beam propagating in the biological tissues has been derived; the properties of an LG vortex beam propagating in the biological tissues have been widely studied by using the numerical examples. It is found that the LG vortex beam will lose the dark hollow center and evolve into a Gaussian-like beam as the propagation distance increases. It is also found that the LG vortex beam propagating in biological tissues with smaller C_n^2 will evolve into a Gaussian-like beam slower. The beam profile of an LG vortex beam propagating in the biological tissues will change as the propagation distance z increases.

REFERENCES

1. Arshad, K., M. Lazar, S. Mahmood, Aman-ur-Rehman, and S. Poedts, "Kinetic study of electrostatic twisted waves instability in nonthermal dusty plasmas," *Physics of Plasmas*, Vol. 24, 033701, 2017.
2. Arshad, K., M. Lazar, and S. Poedts, "Quasi-electrostatic twisted waves in Lorentzian dusty plasmas," *Planetary and Space Science*, Vol. 156, 139–146, 2018.
3. El Gawhary, O. and S. Severini, "Lorentz beams and symmetry properties in paraxial optics," *Journal of Optics A — Pure and Applied Optics*, Vol. 8, 409–414, 2006.
4. Zhao, C. and Y. Cai, "Paraxial propagation of Lorentz and Lorentz-Gauss beams in uniaxial crystals orthogonal to the optical axis," *J. Mod. Optic*, Vol. 57, 375–384, 2010.

5. Liu, D., Y. Wang, G. Wang, and H. Yin, "Influences of oceanic turbulence on Lorentz Gaussian beam," *Optik — International Journal for Light and Electron Optics*, Vol. 154, 738–747, 2018.

6. Yu, H., L. Xiong, and B. Lue, "Nonparaxial Lorentz and Lorentz-Gauss beams," *Optik*, Vol. 121, 1455–1461, 2010.

7. Zhou, G. Q. and X. X. Chu, "Average intensity and spreading of a Lorentz-Gauss beam in turbulent atmosphere," *Opt. Express*, Vol. 18, 726–731, 2010.

8. Du, W., C. L. Zhao, and Y. J. Cai, "Propagation of Lorentz and Lorentz-Gauss beams through an apertured fractional Fourier transform optical system," *Opt. Laser Eng.*, Vol. 49, 25–31, 2011.

9. Zhou, G. and R. Chen, "Wigner distribution function of Lorentz and Lorentz-Gauss beams through a paraxial ABCD optical system," *Appl. Phys. B-Lasers O*, Vol. 107, 183–193, 2012.

10. Liu, D., H. Yin, and G. Wang, "Nonparaxial propagation of a partially coherent Lorentz-Gauss beam," *Optik — International Journal for Light and Electron Optics*, Vol. 155, 190–199, 2018.

11. Liu, D., G. Wang, and Y. Wang, "Average intensity and coherence properties of a partially coherent Lorentz-Gauss beam propagating through oceanic turbulence," *Optics & Laser Technology*, Vol. 98, 309–317, 2018.

12. Ni, Y. Z. and G. Q. Zhou, "Nonparaxial propagation of Lorentz-Gauss vortex beams in uniaxial crystals orthogonal to the optical axis," *Appl. Phys. B-Lasers O*, Vol. 108, 883–890, 2012.

13. Zhou, G. Q. and G. Y. Ru, "Angular momentum density of a linearly polarized Lorentz-Gauss vortex beam," *Opt. Commun.*, Vol. 313, 157–169, 2014.

14. Zhou, G. Q., "Propagation property of a Lorentz-Gauss vortex beam in a strongly nonlocal nonlinear media," *Opt. Commun.*, Vol. 330, 106–112, 2014.

15. Zhou, G. Q., Z. Y. Ji, and G. Y. Ru, "Orbital angular momentum density of a general Lorentz-Gauss vortex beam," *Laser Phys.*, Vol. 26, 075002, 2016.

16. Liu, D., H. Yin, G. Wang, and Y. Wang, "Propagation of partially coherent Lorentz-Gauss vortex beam through oceanic turbulence," *Appl Optics*, Vol. 56, 8785–8792, 2017.

17. Liu, D., H. Zhong, G. Wang, H. Yin, and Y. Wang, "Evolution properties of a partially coherent Lorentz-Gauss vortex beam in a uniaxial crystal," *J. Mod. Optic*, Vol. 66, 1–10, 2019.

18. Liu, X. Y. and D. M. Zhao, "The statistical properties of anisotropic electromagnetic beams passing through the biological tissues," *Opt. Commun.*, Vol. 285, 4152–4156, 2012.

19. Luo, M. L., Q. Chen, L. M. Hua, and D. M. Zhao, "Propagation of stochastic electromagnetic vortex beams through the turbulent biological tissues," *Phys. Lett. A*, Vol. 378, 308–314, 2014.

20. Lu, X. Y., X. L. Zhu, K. L. Wang, C. L. Zhao, and Y. J. Cai, "Effects of biological tissues on the propagation properties of anomalous hollow beams," *Optik*, Vol. 127, 1842–1847, 2016.

21. Liu, D., H. Zhong, and Y. Wang, "Intensity properties of anomalous hollow vortex beam propagating in biological tissues," *Optik*, Vol. 170, 61–69, 2018.

22. Jeffrey, H. D. A., *Handbook of Mathematical Formulas and Integrals*, 4th Edition, Academic Press Inc., 2008.

23. Schmidt, P., "A method for the convolution of lineshapes which involve the Lorentz distribution," *Journal of physics B*, Vol. 9, 2331–2339, 1976.

24. Schmitt, J. and G. Kumar, "Turbulent nature of refractive-index variations in biological tissue," *Opt. Lett.*, Vol. 21, 1310–1312, 1996.